Tunable Nonequilibrium Luttinger Liquid Based on Counterpropagating Edge Channels

M. G. Prokudina,[1] S. Ludwig,[2] V. Pellegrini,[3] L. Sorba,[4] G. Biasiol,[5] and V. S. Khrapai[1,6]
[1]Institute of Solid State Physics, Russian Academy of Sciences, 142432 Chernogolovka, Russian Federation
[2]Center for NanoScience and Fakultät für Physik, Ludwig-Maximilians-Universität, Geschwister-Scholl-Platz 1, D-80539 München, Germany
[3]Istituto Italiano di Tecnologia (IIT), Via Morego 30, 16163 Genova, Italy and NEST, Istituto Nanoscienze-CNR and Scuola Normale Superiore, I-56126 Pisa, Italy
[4]NEST, Istituto Nanoscienze-CNR and Scuola Normale Superiore, Piazza San Silvestro 12, I-56127 Pisa, Italy
[5]CNR-IOM, Laboratorio TASC, Area Science Park, I-34149 Trieste, Italy
[6]Moscow Institute of Physics and Technology, 141700 Dolgoprudny, Russian Federation
(Received 21 January 2014; published 29 May 2014)

We investigate the energy transfer between counterpropagating quantum Hall edge channels (ECs) in a two-dimensional electron system at a filling factor of $\nu = 1$. The ECs are separated by a thin impenetrable potential barrier and Coulomb coupled, thereby constituting a quasi-one-dimensional analogue of a spinless Luttinger liquid (LL). We drive one, say hot, EC far from thermal equilibrium and measure the energy transfer rate P into the second, cold, EC using a quantum point contact as a bolometer. The dependence of P on the drive bias indicates a breakdown of the momentum conservation, whereas P is almost independent of the length of the region where the ECs interact. Interpreting our results in terms of plasmons (collective density excitations), we find that the energy transfer between the ECs occurs via plasmon backscattering at the boundaries of the LL. The backscattering probability is determined by the LL interaction parameter and can be tuned by changing the width of the electrostatic potential barrier between the ECs.

DOI: 10.1103/PhysRevLett.112.216402 PACS numbers: 71.10.Pm, 73.23.-b

One-dimensional electronic systems (1DESs) are collective in nature. As first shown by Tomonaga [1], an interacting 1DES near its ground state can be modeled with the help of a bosonization technique. Later on, Luttinger [2] introduced an exactly soluble [3] model for two species of fermions (left and right movers) with an infinite linear dispersion, referred to as a Luttinger liquid (LL). The excitations of a spinless LL can be described as noninteracting plasmons, bosonic collective fluctuations of the electron density [4]. The plasmon's lack of interaction gives rise to the counterintuitive prediction that an excited ideal LL should never thermalize.

The strength of the LL model fully manifests itself out of equilibrium, where it still offers a single-particle description of the kinetics of a strongly correlated 1DES. In the presence of disorder, energy relaxation is then described as elastic plasmon scattering off inhomogeneities [5,6]. This has not yet been confirmed experimentally. Instead, for two tunnel-coupled quantum wires far from equilibrium deviations from the LL model were observed [7]. The main problem seems to be disorder, which gives rise to thermalization on the length scale of the mean free path [6]. Signatures of disordered LLs, such as a power law dependence of the conductance on temperature or bias, have been observed in various 1DESs [8–10]. However, the design of experiments far from equilibrium remains complicated because of small mean free paths of no more than a few micrometers in such devices [11].

Here we apply a strong magnetic field perpendicular to the two-dimensional electronic system (2DES) of a GaAs/AlGaAs heterostructure and realize a tunable LL based on edge channels (ECs) at an integer filling factor of $\nu = 1$. Related to their chiral nature, ECs offer the fundamental advantage of suppressed backscattering of electrons [12]. Yet, contrary to the chiral LLs in the fractional quantum Hall regime [13], a single EC at $\nu = 1$ behaves as a perfect one-dimensional Fermi liquid [14,15]. To still create a spinless LL we bring two counterpropagating ECs into interaction, providing left and right movers according to the original proposal by Luttinger. Here we follow Ref. [16], where a direct analogy between such a system and the LL model has been demonstrated. Unlike in experiments on tunneling in cleaved edge overgrown [17] and corner-overgrown [18] structures, we block the charge current between the ECs and study the energy transfer between the left and right movers in this handmade LL. Besides much weaker disorder, this system has a second important advantage, namely, the possibility of individual control over left versus right movers.

Our counterpropagating ECs are separated by a barrier impenetrable for electrons, marked by C in Fig. 1(a). It is created electrostatically by applying a negative voltage V_C to the metallic center gate [C in Fig. 1(b)]. Varying V_C allows us to tune the width of the barrier and the strength of the Coulomb coupling between the ECs. Other gates [1 through 8 in Fig. 1(b)] have two purposes: first, they can be

used to control the length of the interaction region (L) by guiding the ECs away from the center barrier. Their second purpose is to define quantum point contacts (QPCs). We create a nonequilibrium electronic distribution in one, say hot, EC by partitioning the electrons at a drive QPC [19,20] [DRIVE circuit in Fig. 1(a)]. Based on this technique, energy relaxation between copropagating ECs was already investigated at $\nu = 2$ with a quantum dot as the detector [20,21] and in the fractional quantum Hall regime by observation of complex edge reconstruction effects [22]. We use a second QPC, defined in the counterpropagating EC [DETECTOR circuit in Fig. 1(a)], to detect the excess energy transferred from the hot EC. This setup allows us to create a perfect LL model system out of equilibrium and to study the energy flux between the left and right movers (red winding arrows in Fig. 1(a).

Our samples are based on a 200 nm deep 2DES of a GaAs/AlGaAs heterostructure with electron density 9.3×10^{10} cm^{-2} and mobility 4×10^6 cm^2/Vs. The metallic gates are obtained by thermal evaporation of 3 nm Ti and 30 nm Au. The experiments are performed in a ^{3}He/^{4}He dilution refrigerator in a magnetic field of 3.8 T at 60 and 90 mK. Current measurements are performed using homemade I–V converters with an input offset voltage $\lesssim 10$ μV. In bolometric experiments, the detector QPC conductance is measured with a 5 μV rms ac modulation (11—33 Hz). For thermoelectric measurements we use a fixed ac modulation (11—33 Hz) and measure the derivative $dI_{\rm DET}/dV_{\rm DRIVE}$ as a function of the dc bias $V_{\rm DRIVE}$, which is numerically integrated to give $I_{\rm DET}$. The modulation is 5 μV rms at $|V_{\rm DRIVE}| \leq 300$ μV, and 30 μV rms otherwise. Throughout the Letter the drive QPCs conductance is $\approx 0.3e^2/h$, corresponding to a perfectly linear I–V. Hence, the excitation is the same for both polarities of $V_{\rm DRIVE}$, explaining an almost perfect symmetry of the data in Figs. 2 and 3 below.

The linear response conductance of a QPC, $G = {\rm Tr} \times e^2/h$, is proportional to its transparency Tr, the probability for an electron to be transmitted through the QPC. The energy dependence of Tr can be used to convert a thermal gradient into an electric current [24,26,27]. Here we demonstrate a simpler and quantitative approach and use a QPC as a bolometer. In leading order $\delta G_{\rm DET}$ is proportional to the excess energy fluxes δF_L and

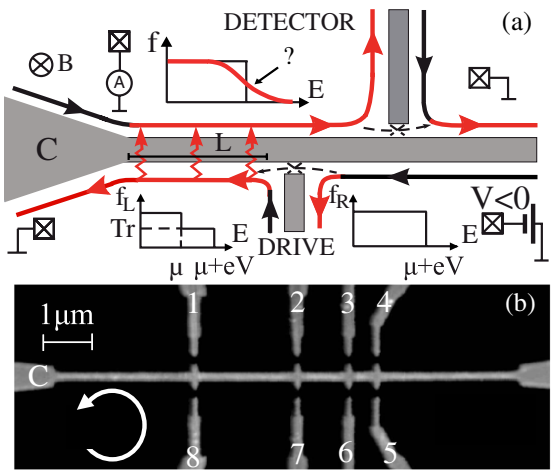

FIG. 1 (color online). Experimental layout. (a) Gated areas of the 2DES are shown in gray and the ECs are shown by solid lines with arrows. In the drive circuit we create a nonequilibrium particle distribution in a hot EC by using a partially transparent drive QPC biased with a voltage $V_{\rm DRIVE}$. The hot EC propagates along the central barrier (C), reaches the interaction region of length L and heats a counterpropagating cold EC in the detector circuit (winding arrows). The nonequilibrium distribution in the cold EC is characterized with the help of the detector QPC. (b) Electron micrograph of the sample identical to the one used in the experiment. The central gate (C) and a number of side gates used to define constrictions have a gray color. The EC chirality is the same as in (a), see the white arrow.

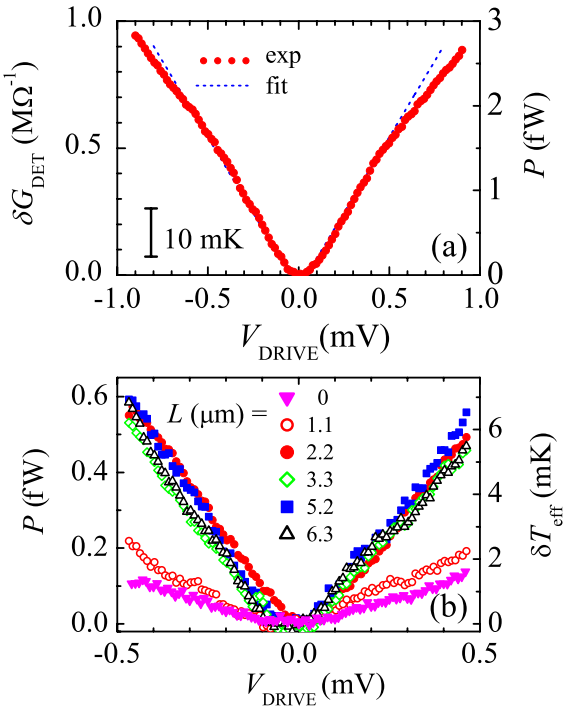

FIG. 2 (color online). QPC as a bolometer. (a) Bolometric response $\delta G_{\rm DET}$ versus $V_{\rm DRIVE}$ (dots). The detector QPC is defined by gate 2 and the drive QPC with gate 5, $L = 5.2$ μm. The energy transfer rate P is shown on right axis scale. The vertical scale bar corresponds to $\delta T_{\rm eff} = 10$ mK. The dashed line is a fit to the model of boundary plasmon scattering with parameters $\epsilon_0 = 80$ μeV, $K \approx 1.12$. The data were taken at $V_C = -0.6$ V and $T = 60$ mK. (b) P (left axis) and $\delta T_{\rm eff}$ (right axis) as a function of $V_{\rm DRIVE}$ for various values of L (see legend). The detector QPC is defined with gate 2 (closed symbols) or gate 3 (open symbols). The drive QPC is placed about 40 μm upstream of the interaction region [not shown in Fig. 1(b)]. For this data, the electrostatic contribution was subtracted [23]. $\delta G_{\rm DET}$ and P are considerably smaller than in Fig. 2(a), because of the hot EC cooling down on the way to the interaction region [24]. The data were taken at $V_C = -0.385$ V and $T = 90$ mK.

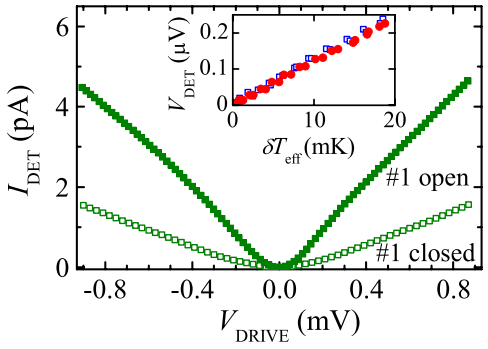

FIG. 3 (color online). Thermoelectric measurements. I_{DET} across the detector QPC 2 excited with the help of the drive QPC 8, $L = 3$ μm. The sign of I_{DET} corresponds to the injection of nonequilibrium electrons across the detector QPC, similar to the case of small magnetic fields [25]. The effect is reduced when gate 1 is closed and the interaction region is isolated from the detector QPC, $L = 0$ [Fig. 1(b)]. Inset: Proportionality of V_{DET} and δT_{eff} in the detector EC measured with the drive QPCs 5 (closed dots) and 6 (open squares) and detector QPC 2, $L = 5.2$ μm. All the data corresponds to $V_C = -0.6$ V and $T = 60$ mK.

δF_R impinging on it, respectively, from the left and right, and the second energy derivative of Tr:

$$\delta G_{DET} = e^2 \frac{\partial^2 \mathrm{Tr}_{DET}}{\partial E^2} \frac{\delta F_R + \delta F_L}{2}. \quad (1)$$

In the measurements discussed below, we use either gate 2 or gate 3 [Fig. 1(b)] to define our detector QPC at $\mathrm{Tr}_{DET} \simeq 0.1$.

In Fig. 2(a) we present a typical bolometer measurement of δG_{DET} versus V_{DRIVE}. δG_{DET} is parabolic at small $|V_{DRIVE}|$ and close to linear for $|V_{DRIVE}| \gtrsim 100$ μV. $\delta G_{DET}(V_{DRIVE})$ is nearly symmetric with respect to the origin, indicating that the excess energy in the hot EC is independent of the sign of V_{DRIVE}. Similar results are obtained when the drive QPC is placed 40 μm upstream of the interaction region; see Fig. 2(b). We verified that our bolometer indeed probes the energy transfer rate (P) between the ECs within the interaction region. Corresponding experiments and the derivation of formula (1) are presented in the Supplemental Material [28].

We calibrate the bolometer by measuring the temperature T dependence $\partial G_{DET}/\partial T$ in equilibrium and extracting $\partial^2 \mathrm{Tr}_{DET}/\partial E^2$. These two quantities are related via Eq. (1) and a standard expression for the energy flux in equilibrium, $F_R = F_L = \pi^2 (k_B T)^2/6h$ [21]. So obtained P is given on the right and left axes in Figs. 2(a) and 2(b), respectively. P is in the fW range, meaning that just a tiny fraction ($\sim 10^{-4}$) of the excess energy of the hot EC is absorbed in the cold EC. It is tempting to determine an effective excess temperature δT_{eff} in the cold EC. For small changes one finds $\delta T_{eff} = 2\delta G_{DET}/(\partial G_{DET}/\partial T) \ll T$. Here the factor of 2 accounts for the fact that in our experiment $\delta F_L = P$ and $\delta F_R = 0$. δT_{eff} is quantified in Figs. 2(a) (bar) and 2(b) (right axis).

Nonzero δT_{eff} in the cold EC generates a thermoelectric current (I_{DET}) across the detector QPC. In Fig. 3, I_{DET} is plotted against V_{DRIVE} for two choices of L. These data closely resemble the bolometric response shown in Fig. 2, which is a general feature of our measurements. The connection between the two experiments becomes evident in the inset of Fig. 3. The thermoelectric voltage, defined as $V_{DET} \equiv I_{DET}/G_{DET}$, is proportional to δT_{eff} measured using the bolometer. The Seebeck coefficient of the detector QPC $S = \delta V_{DET}/\delta T_{eff} \approx 13$ μV/K is comparable to previous measurements [26,27]. It is independent of the sign of V_{DRIVE} and the choice of the drive QPC, as expected. The meaningful value of S indicates that the cold EC is close to local thermal equilibrium and justifies our bolometric approach.

An observation of $P \propto V_{DRIVE}$ points at a breakdown of the momentum conservation for the energy exchange between counterpropagating ECs [29]. For a deeper analysis we use the kinetic equation approach [5] and express P in an inhomogeneous LL as

$$P = \frac{1}{h} \int \varepsilon f^{HOT}(\varepsilon) R_\varepsilon d\varepsilon, \quad (2)$$

where R_ε is the energy dependent backscattering probability of plasmons and $f^{HOT}(\varepsilon)$ is their occupation number in the hot EC. In the limit of $|\mathrm{eV}_{DRIVE}| \gg k_B T$, ε we can assume $f^{HOT}(\varepsilon) \propto |\mathrm{eV}_{DRIVE}|/\varepsilon$. Hence $P \propto |V_{DRIVE}|$ indicates that backscattering is suppressed at high ε. Such a behavior is expected in a random disorder model with a finite correlation length l_{corr} [30]. The disorder potential absorbs momenta up to $\hbar l_{corr}^{-1}$ and enables transfer of energy quanta up to $\varepsilon_0 \sim \hbar u l_{corr}^{-1}$, where u is the plasmon velocity [31]. With the magnetoplasmon velocity at $\nu = 1$ estimated to be $u \sim 10^7$ cm/s [32] and with $\varepsilon_0 \sim 80$ μeV determined from the onset of the linear slope of $P(V_{DRIVE})$ in Fig. 2(a), we find $l_{corr} \sim 1$ μm for our device.

We gain more insights about plasmon scattering by studying P in dependence on the ECs interaction length L. Using a fixed drive QPC (40 μm upstream of the interaction region) we vary L in the range 0–6.3 μm by bending the hot EC with gates 6, 7, or 8 [see Fig. 1(b)]. As shown in Fig. 2(b), P stays constant as L is increased between 2.2 and 6.3 μm. Obviously, this is inconsistent with random disorder scattering, for which $R_\varepsilon \propto L$ [30]. Moreover, the heretical conclusion that part of the interaction region might be broken and would therefore not contribute to scattering is disproved in Fig. 3. Instead, the independence of P on L indicates boundary scattering of plasmons at the entrance and exit of the interaction region as a dominant energy transfer mechanism. As seen from Fig. 2(b), P depends on L only for small $L \lesssim l_{corr}$, which

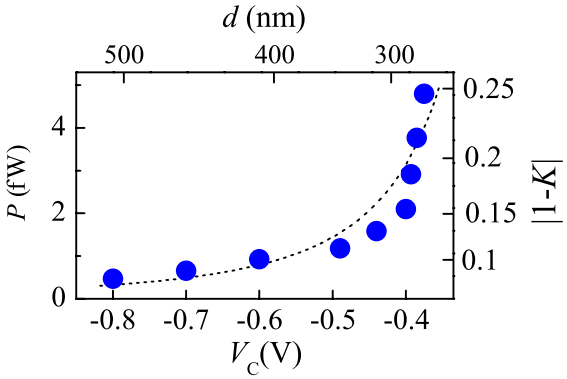

FIG. 4 (color online). Tuning the interaction. P against V_C [Fig. 1(b)] for fixed $V_{\mathrm{DRIVE}} = -0.4$ mV and $T = 90$ mK. Gates 2 and 8 define the detector and drive QPCs, $L = 3$ μm. From the left to the right, the ECs' separation d reduces and K is detuned from its noninteracting value 1 (see the scale on the right). d obtained from a solution of the electrostatic problem is shown on the upper abscissae (see Supplemental Material [28] for the details). The dashed line is a fit with parameters $v_F = 1.2 \times 10^7$ cm/s and $l_{\mathrm{bound}} = 770$ nm, see text.

can be qualitatively explained by an overlap of the two boundaries and a sufficiently long-ranged interaction between the ECs (finite signal at $L = 0$, see also Fig. 3).

The boundary scattering is related to the change of the plasmon velocity in the interaction region, where it is renormalized as $u = v_F/K$. Here v_F is the Fermi velocity in the isolated EC and $K \geq 1$ is a dimensionless LL interaction constant [5]. Note that this process is a plasmon counterpart of a charge fractionalization at the LL boundary [33]. At small energies the scattering obeys the Fresnel law $R_\varepsilon = [(1-K)/(1+K)]^2$. If K varies smoothly across the length scale l_{bound}, the reflection is suppressed for $\varepsilon \gtrsim \varepsilon_0 = \hbar u l_{\mathrm{bound}}^{-1}$, where $l_{\mathrm{bound}} \sim 1$ μm replaces l_{corr} considered above.

An independent indication for boundary scattering is the observed $P \propto V_{\mathrm{DRIVE}}^2$ at weak driving $|\mathrm{eV}_{\mathrm{DRIVE}}| \lesssim \varepsilon_0$; see Fig. 2. This is expected for boundary scattering at $\varepsilon < \varepsilon_0$, as R_ε is constant in this case. In contrast, for disorder scattering [30] $R_\varepsilon \propto \varepsilon^2$ for $\varepsilon < \varepsilon_0$, which would result in $P \propto V_{\mathrm{DRIVE}}^4$, similar to a perturbative calculation [29].

The dashed line in Fig. 2(a) is a model curve based on Eq. (2) assuming boundary scattering of plasmons. The only fit parameters are $\varepsilon_0 = 80$ μeV, which sets the crossover from parabolic to linear $P(V_{\mathrm{DRIVE}})$ and $K = 1.12$. The interaction strength $|1-K|$ can be directly tuned by V_C. As shown in Fig. 4 for the case of $|\mathrm{eV}_{\mathrm{DRIVE}}| \gg \varepsilon_0$, P sharply increases in the range -0.8 V $< V_C < -0.37$ V, corresponding to $0.1 < |1-K| \lesssim 0.25$.

At our largest interaction $u \approx 0.75 v_F$, which corresponds to a dimensionless LL conductance of $g \approx 0.5$. This is close to values reported in genuine 1DESs [7–9]. We finally note that the electrostatic width of the central barrier is $d \simeq 300$ nm (see the upper axis of Fig. 4), comparable to the depth of the 2DES and the width of gate C. Our experiments are in the regime $d < l_{\mathrm{bound}}$, for which the interaction is dominated by Coulomb coupling [29]. We obtain a reasonable agreement (dashed line in Fig. 4) evaluating the interaction as [4] $K = [1 - (g_2/2\pi\hbar v_F)^2]^{-1/2}$, where $g_2 = 2e^2 K_0(qd)/k$ is a matrix element of the Coulomb interaction at a wave vector $q = l_{\mathrm{bound}}^{-1}$, K_0 is the Bessel function and $k \approx 12.5$ is the dielectric constant [34].

In summary, we studied the LL model out of thermal equilibrium based on counterpropagating quantum Hall ECs. The energy transfer between the ECs is consistent with elastic backscattering of collective density excitations at the boundaries of this handmade LL. Counterpropagating quantum Hall ECs are a perfect candidate for refined tests of the LL theory, a first example being presented here.

We are grateful to I. V. Gornyi, I. S. Burmistrov, V. T. Dolgopolov, D. A. Bagrets, and D. V. Shovkun for discussions and to J. P. Kotthaus for his input on the early stages of this work. Financial support from RAS, RFBR Grant No. 12-02-00573, the Ministry of Education and Science of the Russian Federation Grant No. 14Y.26.31.0007, as well as the German Excellence Initiative via the Nanosystems Initiative Munich (NIM) is acknowledged.

Note added in Proof.—After submission of this Letter an experiment studying charge fractionalization in a similar handmade LL system was published by Kamata *et al.* in [35].

[1] S. Tomonaga, Prog. Theor. Phys. **5**, 544 (1950).
[2] J. M. Luttinger, J. Math. Phys. (N.Y.) **4**, 1154 (1963).
[3] D. C. Mattis and E. H. Lieb, J. Math. Phys. (N.Y.) **6**, 304 (1965).
[4] T. Giamarchi, *Quantum Physics in One Dimension* (Oxford University Press, Oxford, 2004).
[5] D. B. Gutman, Yuval Gefen, and A. D. Mirlin, Phys. Rev. B **80**, 045106 (2009).
[6] D. A. Bagrets, I. V. Gornyi, and D. G. Polyakov, Phys. Rev. B **80**, 113403 (2009).
[7] G. Barak, H. Steinberg, L. N. Pfeiffer, K. W. West, L. Glazman, F. von Oppen, and A. Yacoby, Nat. Phys. **6**, 489 (2010).
[8] M. Bockrath, D. H. Cobden, J. Lu, A. G. Rinzler, R. E. Smalley, L. Balents, and P. L. McEuen, Nature (London) **397**, 598 (1999).
[9] O. M. Auslaender, A. Yacoby, R. de Picciotto, K. W. Baldwin, L. N. Pfeiffer, and K. W. West, Phys. Rev. Lett. **84**, 1764 (2000).
[10] P. Segovia, D. Purdie, M. Hengsberger, and Y. Baer, Nature (London) **402**, 504 (1999).
[11] J.-C. Charlier, X. Blase, and S. Roche, Rev. Mod. Phys. **79**, 677 (2007).
[12] M. Büttiker, Phys. Rev. B **38**, 9375 (1988).

[13] A. M. Chang, L. N. Pfeiffer, and K. W. West, Phys. Rev. Lett. **77**, 2538 (1996); M. Grayson, D. C. Tsui, L. N. Pfeiffer, K. W. West, and A. M. Chang, *ibid.* **80**, 1062 (1998); M. Grayson, D. C. Tsui, L. N. Pfeiffer, K. W. West, and A. M. Chang, *ibid.* **86**, 2645 (2001).

[14] M. P. A. Fisher and L. I. Glazman in *Mesoscopic Electron Transport*, NATO ASI Series E, edited by L. Kowenhoven, G. Schoen, and L. Sohn, (Kluwer Academic Publishers, Dordrecht, 1997).

[15] M. Hilke, D. C. Tsui, M. Grayson, L. N. Pfeiffer, and K. W. West, Phys. Rev. Lett. **87**, 186806 (2001).

[16] Y. Oreg and A. M. Finkel'stein, Phys. Rev. Lett. **74**, 3668 (1995).

[17] W. Kang, H. L. Stormer, L. N. Pfeiffer, K. W. Baldwin, and K. W. West, Nature (London) **403**, 59 (2000).

[18] M. Grayson, L. Steinke, D. Schuh, M. Bichler, L. Hoeppel, J. Smet, K. v. Klitzing, D. K. Maude, and G. Abstreiter, Phys. Rev. B **76**, 201304(R) (2007); L. Steinke, D. Schuh, M. Bichler, G. Abstreiter, and M. Grayson, *ibid.* **77**, 235319 (2008); L. Steinke, P. Cantwell, D. Zakharov , E. Stach, N. J. Zaluzec, A. Fontcuberta i Morral, M. Bichler, G. Abstreiter, and M. Grayson, Appl. Phys. Lett. **93**, 193117 (2008).

[19] B. J. van Wees, L. P. Kouwenhoven, H. van Houten, C. W. J. Beenakker, J. E. Mooij, C. T. Foxon, and J. J. Harris, Phys. Rev. B **38**, 3625 (1988).

[20] H. le Sueur, C. Altimiras, U. Gennser, A. Cavanna, D. Mailly, and F. Pierre, Phys. Rev. Lett. **105**, 056803 (2010).

[21] C. Altimiras, H. le Sueur, U. Gennser, A. Cavanna, D. Mailly, and F. Pierre, Nat. Phys. **6**, 34 (2010).

[22] V. Venkatachalam, S. Hart, L. Pfeiffer, K. West, and A. Yacoby, Nat. Phys. **8**, 676 (2012).

[23] The trivial electrostatic contribution to G_{DET} arises from the change of the electron density in the biased drive circuit owing to the in-plain gating effect. For $|\delta G_{\mathrm{DET}}/G_{\mathrm{DET}}| \ll 1$ it is asymmetric in drive bias $\delta G_{\mathrm{DET}} \propto V_{\mathrm{DRIVE}}$. This contribution was independently calibrated in experiments with an open drive QPC, when the bolometric contribution is absent.

[24] G. Granger, J. P. Eisenstein, and J. L. Reno, Phys. Rev. Lett. **102**, 086803 (2009).

[25] M. G. Prokudina, V. S. Khrapai, S. Ludwig, J. P. Kotthaus, H. P. Tranitz, and W. Wegscheider, Phys. Rev. B **82**, 201310 (R) (2010).

[26] L. W. Molenkamp, Th. Gravier, H. van Houten, O. J. A. Buijk, M. A. A. Mabesoone, and C. T. Foxon, Phys. Rev. Lett. **68**, 3765 (1992).

[27] A. S. Dzurak, C. G. Smith, L. Martin-Moreno, M. Pepper, D. A. Ritchie, G. A. C. Jones, and D. G. Hasko, J. Phys. Condens. Matter **5**, 8055 (1993).

[28] See Supplemental Material at http://link.aps.org/supplemental/10.1103/PhysRevLett.112.216402 for cross-check experiments, derivation of Eq. (1) and details of fitting procedure.

[29] M. G. Prokudina and V. S. Khrapai, JETP Lett. **95**, 345 (2012).

[30] A. Gramada and M. E. Raikh, Phys. Rev. B **55**, 7673 (1997).

[31] A. M. Lunde, S. E. Nigg, and M. Buttiker, Phys. Rev. B **81**, 041311(R) (2010).

[32] N. B. Zhitenev, R. J. Haug, K. v. Klitzing, and K. Eberl, Phys. Rev. Lett. **71**, 2292 (1993); H. Kamata, T. Ota, K. Muraki, and T. Fujisawa, Phys. Rev. B **81**, 085329 (2010).

[33] D. L. Maslov and M. Stone, Phys. Rev. B **52**, R5539 (1995); I. Safi and H. J. Schulz, *ibid.* **52**, R17040 (1995); V. V. Ponomarenko, *ibid.* **52**, R8666 (1995).

[34] At $|K-1| \ll 1$ a renormalization of the plasmon velocity is small, and we expect a perturbative description to be adequate as well. Unlike in Ref. [29], in this case one has to account for a pairwise electron-electron scattering at the boundaries of the interaction region.

[35] H. Kamata, N. Kumada, M. Hashisaka, K. Muraki, and T. Fujisawa, Nat. Nanotechnol. **9**, 177 (2014).